

---

## **Fracture surface analysis of AA2218 Al-alloy MMCs and squeeze pressure effect on fracture mechanism**

---

Amneesh Singla\* and Yashvir Singh

Department of Mechanical Engineering,  
University of Petroleum and Energy Studies,  
Dehradun, Uttarakhand, 248007, India  
Email: amneesh82@gmail.com  
Email: yashvirsingh21@gmail.com

\*Corresponding author

**Abstract:** A novel stir casting technique have been used for the development of AA2218-based metal matrix composite with the reinforcement of Al<sub>2</sub>O<sub>3</sub> (TiO<sub>2</sub>) particles. Coarser Al<sub>2</sub>O<sub>3</sub> and finer TiO<sub>2</sub> particles are ball milled together after mixing in different proportion to achieve coating of the coarser particles by the finer one to promote wettability. The composite have been prepared by the addition of ball milled powder by 2% and 5% weight fraction in an aluminium melt. The developed as cast composites have been artificially aged using T61 heat treatment at 510°C for 4 hours and peak aging at 170°C for 10 h followed by squeeze cast between 100–220 MPa pressure. Tensile studies have been conducted on the specimens. Hardness and tensile strength is increased by adding alumina and TiO<sub>2</sub>. The improvement in ductility has been observed after aging at higher squeeze pressure. The fractured surfaces of tensile test specimens have been analysed and mechanism of fracture along with the effect of squeeze pressure and effect of particle wt% has been discussed.

**Keywords:** metal matrix composites; MMCs; stir casting; squeeze pressure; heat treatment; fracture.

**Reference** to this paper should be made as follows: Singla, A. and Singh, Y. (xxxx) 'Fracture surface analysis of AA2218 Al-alloy MMCs and squeeze pressure effect on fracture mechanism', *Int. J. Materials Engineering Innovation*, Vol. X, No. Y, pp.xxx–xxx.

**Biographical notes:** Amneesh Singla is a Mechanical Engineer with Masters in Mechanical Engineering, and is pursuing a PhD in metal matrix composites area. Since 2004, he has been involved in teaching and research. He taught various subjects related to materials. He is working as Assistant Professor in the Mechanical Engineering Department of the University of Petroleum and Energy Studies, Dehradun.

Yashvir Singh is a Mechanical Engineer with Masters in Mechanical Engineering, and is pursuing a PhD in tribological behaviour area. Since 2007, he has been involved in teaching and research. He taught various subjects related to tribology. He is working as Assistant Professor in the Mechanical Engineering Department of the University of Petroleum and Energy Studies, Dehradun.

## 1 Introduction

Metal matrix composites (MMCs) are man-made materials that can be synthesised with predetermined properties. MMCs have shown promising industrial applications in light weight and high performance area. Due to the variety of application and importance of MMCs, a lot of MMC fabrication techniques have been developed during the last previous years. The particle reinforced MMCs can be produced through melt process and powder metallurgy process (Seo and Kang, 1995; Sahin et al., 2002). The PMMCs are of particular interest due to their ease of fabrication by conventional methods and lower costs and flexibility. As compared to the powder metallurgy route, the liquid phase process is more preferable due to better matrix-particle bonding and easier control of mixture structure (Seo and Kang, 1995; Sahin et al., 2002; Ray, 1993; Hanumant and Irons, 1993). However, liquid phase processing has two main problems – first is the wettability problem of ceramic particles with melt matrix and second the non-uniform dispersion of ceramic particles due to the density difference (Lafreniene and Irons, 1990; Asthana and Rohtagi, 1992). The wetting behaviour is characterised by the contact angle between alumina and molten aluminium. Generally, alumina is not wettable by molten aluminium due to the contact angle which is greater than 90°. The great effort has been made by researcher to determine the wettability between solid alumina and molten aluminium (Wang and Wu, 1994; Naidich et al., 1983). Aluminium-based MMC have often been reinforced by the addition of ceramic particles like Al<sub>2</sub>O<sub>3</sub> (Quigley et al., 1982; Kang and Yun, 1996; Hamid et al., 2006; Abis, 1989), SiC (Davidson and Regener, 2000; Ralph et al., 1997; Surappa and Rohatgi, 1981), TiC (Tjong and Mai, 2008), and TiO<sub>2</sub> (Maity et al., 1993, 1995; Wang et al., 2004), etc.

In the past decades, fracture behaviour studies of MMCs have become one of the major areas of interest (Kumar et al., 2014). The study of various parameters like fabrication method, specification of material, tensile loading etc. which affect the fracture behaviour have become an active field.

Al<sub>2</sub>O<sub>3</sub> is an ideal particle for reinforcement in aluminium and in its alloys because of its good compatibility with aluminium matrix. Apart from this, it is easily available and cost is low. AA2218 Al-alloy being a 2xxx series alloy is heat treatable and it is also known for its elevated temperature applications. It retains about 50% of its tensile strength (TS) at 200°C as compared to ambient temperature. Typical applications of AA2218 Al-alloy are in forged cylinder heads and pistons (Lampman and Theodore, 2000). Two common heat treatments are given to AA2218 Al-alloy:

- 1 T61 (solutionising and peak aging)-solutionising at 510°C (950°F) for 4 h followed by cold water quenching and then artificial aging (precipitation heat treatment) at 170°C (340°F) for 10 h followed by air cooling (Chandler, 1996)
- 2 T72 (solutionising and stabilising)-solutionising at 510°C (950°F) for 4 h followed by cold water quenching and then stabilising at 240°C (460°F) for 6 h followed by air cooling (Dunn et al., 1975).

The density of AA2218 is 2.8 g/cc, solidus temperature is 532°C (990°F) and liquidus temperature is 635°C (1175°F).

Very little work have been carried out on 2218AA in past. In the present investigation, to promote wettability alumina particle have been coated with TiO<sub>2</sub> by ball milling operation. Also, the metal stirring method has been used to obtain the uniform

distribution of ceramic particles in the molten metal. In this study, the effect of wt % reinforced particle and squeeze pressure have been examined to understand the fracture behaviour.

## 2 Experimental setup

Table 1 shows the AA 2218 compositions used for the study. The Powder mixture of coarser  $\text{Al}_2\text{O}_3$  (53–75  $\mu\text{m}$ ) and finer  $\text{TiO}_2$  particles (25–53  $\mu\text{m}$ ) were separated by sieving from the as received position. To remove the moisture and the gases, the powder was heated for 2 hours at 873°C. Heat treated  $\text{Al}_2\text{O}_3$  and  $\text{TiO}_2$  powders ball milled together in the ratio of 1:2 on the basis of rough calculation and rigorously agitated for about 30–35 minutes in an effort to coat the coarser particles by the finer ones to promote wetting of alumina. The injection of  $\text{Al}_2\text{O}_3$  and  $\text{TiO}_2$  particles increases the fracture toughness as the layer of  $\text{TiO}_2$  particles cladded on  $\text{Al}_2\text{O}_3$  particles during milling process (Pawlowski, 1995). This binary mixed oxide offers an attractive combination of corrosion resistance, mechanical strength and interfacial adhesion (Curran and Clyne, 2005). The ball mill used in the present study has a stainless steel chamber with different ball size diameters. Now the ceramic particles reinforced externally inmelt alloy based on AA2218 Al-alloy using stir casting technique.

**Table 1** Element composition of 2218 alloy (mass %)

<i>Cu</i>	<i>Si</i>	<i>Ni</i>	<i>Mg</i>	<i>Mn</i>	<i>Zn</i>	<i>Al</i>
3.76	1.25	1.25	1.08	0.5	0.23	Bal.

TS of AA2218-T72 alloy at ambient temperature is 48000 psi whereas for T61 it is 59,000 psi and yield strength for T61 treated alloy is 74.5% of TS at ambient temperature. BHN (Brinell hardness number) at 500 kg load with 10 mm indenter ball diameter is 115 for AA2218-T61 and 95 for AA2218-T72 (Hamid et al., 2006). Therefore, it has been decided to give T61 treatment (solutionising at 510°C for 4 h and peak aging at 170°C for 10 h) to the composites in present investigation (Abis, 1989). Two different composites have been prepared namely; AA2218-2 wt%  $\text{Al}_2\text{O}_3$  ( $\text{TiO}_2$ ) and AA2218-5 wt%  $\text{Al}_2\text{O}_3$  ( $\text{TiO}_2$ ). The melt-particle slurry has been cast using stir casting in which turbine impeller type of stirrer has been employed. The composites with 5 wt% particle mix have been squeeze cast at 100, 140, 180, 200 and 220 MPa by first pouring superheated alloy-particle stirred slurry in a die and then, immediately transferring the die on the bed of hydraulic press. Optical microscopy has been used to examine microstructures of polished specimens of composites in etched condition. Microstructures have been examined using Leica-DMI 5000 M inverted digital microscope; make Leica Microsystems, Wetzlar, Germany. Etching has been done with Keller's reagent (1.25 ml  $\text{HNO}_3$ , 0.75 ml  $\text{HCl}$ , 0.5 ml  $\text{HF}$  and 47.5 ml  $\text{H}_2\text{O}$ , applied for 40 s).

Tensile studies have been also conducted at elevated temperature up to 400°C (673 K) for 5 wt% MMCs. The specimens have been machined out from the cylindrical cast ingots of gravity cast and squeeze cast composites in peak aged and solutionised conditions. Composites have been tested under uniaxial tension on a computerised Electronic Tensometer PC 2000 (Hounsfield type, make-Kudale Instruments Pvt. Ltd., Pune, India) at an extension rate 1 mm/min. At least three standard tensile specimens of

5.0 mm gauge diameter and 25 mm gauge length as per ASTM E 8M-89b have been machined out from each section of cast ingot and tested. In present study, the fractured surfaces of tensile test specimens have been analysed and mechanism of fracture along with the effect of squeeze pressure and increase in particle wt% has been discussed. Fractured surfaces of tensile specimen have been examined by FE-SEM with EDAX model QUANTA 200 FEG (make-FEI, Netherlands) with resolution 2 nm, HV 200 V – 30 kV.

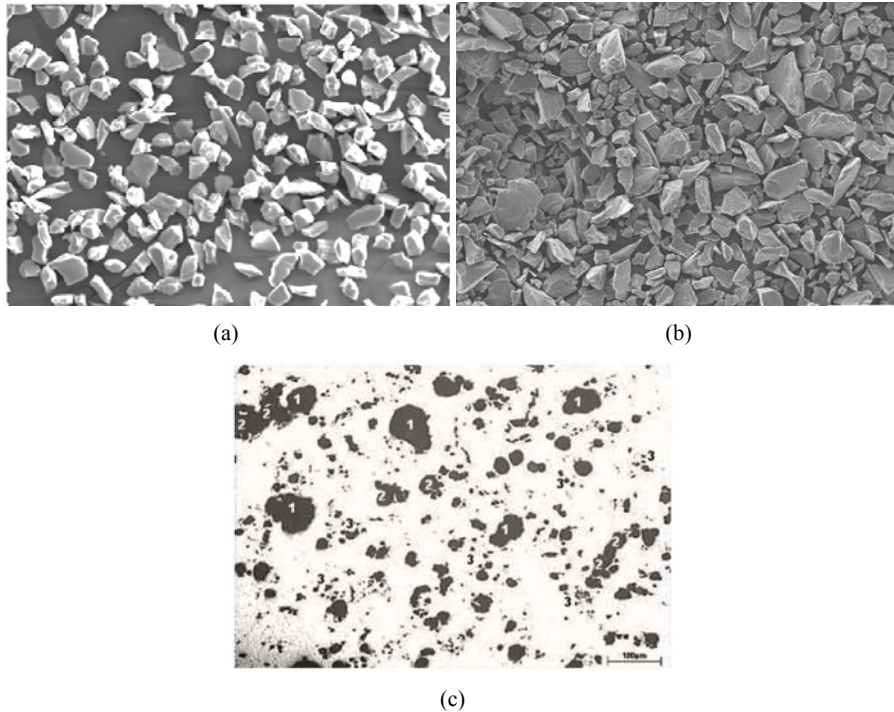
### 3 Results and discussion

Figures 1(a) and 1(b) shows the SEM images of the  $Al_2O_3$  and  $TiO_2$  powder in as received state respectively. Figure 1(c) shows the microstructure of ball milled powder before the addition to the alumina alloy melt for making composite. Microstructure shows the three different sizes of particles:

- 1 large alumina particles with fine particles of  $TiO_2$  adhering to them
- 2 midsize particles formed during milling process
- 3 fine particles formed by oxidation during the process.

All the above three sizes is marked in Figure 1 as 1, 2 and 3.

**Figure 1** (a) shows SEM image of as received  $Al_2O_3$  powder (b) Shows SEM image of as received  $TiO_2$  powder (c) Microstructure of  $Al_2O_3$  ( $TiO_2$ ) ball milled powder at 50×



Typical etched microstructures of AA2218-2 wt%  $\text{Al}_2\text{O}_3$  ( $\text{TiO}_2$ )-T61 composite gravity cast at 500 $\times$  is shown in Figure 2.

**Figure 2** Shows typical etched microstructures of AA2218-2 wt%  $\text{Al}_2\text{O}_3$  ( $\text{TiO}_2$ )-T61 composite gravity cast at 500 $\times$

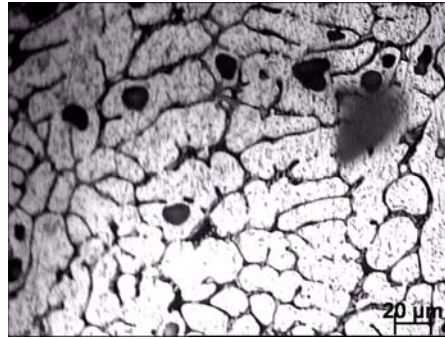


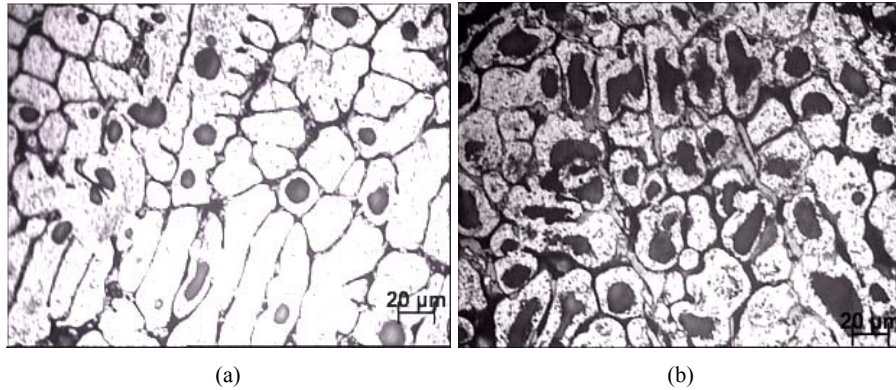
Figure 2 reveals that the cell size of the dendrites are of the order of magnitude lower than the larger particles but the smaller particles are sometimes within the cell, embedded in primary solid solution of aluminium. Small particles embedded in the primary phase within the cells are also observed which may have trapped in the last freezing zone, being pushed by progressing solid-liquid interface.

It may be observed that the composites synthesised by addition of 5 wt% blended particles has relatively more particles compared to that observed in the microstructures of gravity cast AA2218-2 wt%  $\text{Al}_2\text{O}_3$  ( $\text{TiO}_2$ )-T61 aged composite as shown in Figure 2(a). This is indicative of the role of some of the smaller particles of  $\text{TiO}_2$  in nucleating dendritic solidification, which is evident from these particles occurring within the dendrite cells. Composite in which 5 wt% particles have been added, contains more particles than composite in which 2 wt% particles have been added, which is very much expected also as  $\text{TiO}_2$  is reported to undergo chemical reaction with Al in the alloy matrix to form  $\text{Al}_2\text{O}_3$  particles of very small size and Ti, which goes into the alloy (Dunn et al., 1975; Lawson, 1971). These particles embedded within the cells are relatively finer and may have originated primarily from  $\text{TiO}_2$  particles or during processing from the alloy.

On comparing Figures 3(a) and 3(b), it can be observed that with increase in squeeze pressure from 0 MPa (gravity cast) to 220 MPa, the dendrite cell size decreases. It is also observed that the dendrite cell boundaries have become thicker and finer with the increase in squeeze pressure. Increase in number of particles embedded within the cells also appears to be more in composites squeezed at higher pressures. The cells become more circular with increasing squeeze pressure as observed clearly by comparing microstructures in Figures 3(a) and 3(b).

During the tensile property study, it has been found that with the increase of squeeze pressure, ultimate tensile strength (UTS) of the specimen also increases. The UTS without application of squeeze pressure was 250 MPa and as the squeeze pressure increases from 140 to 220 MPa, the observed values of UTS were 295 and 425 MPa respectively.

**Figure 3** Typical etched optical micrographs of AA2218-Al<sub>2</sub>O<sub>3</sub> (TiO<sub>2</sub>)-T61 aged composites synthesised by addition of 5 wt% blended powder at 500 $\times$ , (a) gravity cast, (b) squeeze cast at pressure 220 MPa



The number of particles engulfed by the dendrite cells is more as compared to the number of particles trapped in between the dendrite cells in squeeze cast composites, as shown in Figure 2(b), which can be directly correlated to increasing number of cells with increase in squeeze pressure and lesser time for the particles to segregate along the cell boundary. Decreasing cell size and increasing particle content within dendrites may be indicative of faster solidification at increasing squeeze pressure as reported for squeeze casting in literature (Yue, 1997; Yue and Chadwick, 1996; Kim et al., 2001; Khair and Abou, 2005).

This may be due to increasing heat transfer coefficient across metal-mould interface. The thickness of the gap at the mould-metal interface may reduce due to increased squeeze pressure. It could be due to quicker freezing resulting in higher speed of dendrite solidification front leading to larger particle entrapment within the primary phase. This may have favourable impact on mechanical properties and wear behaviour of squeeze cast composites as compared to gravity cast composites.

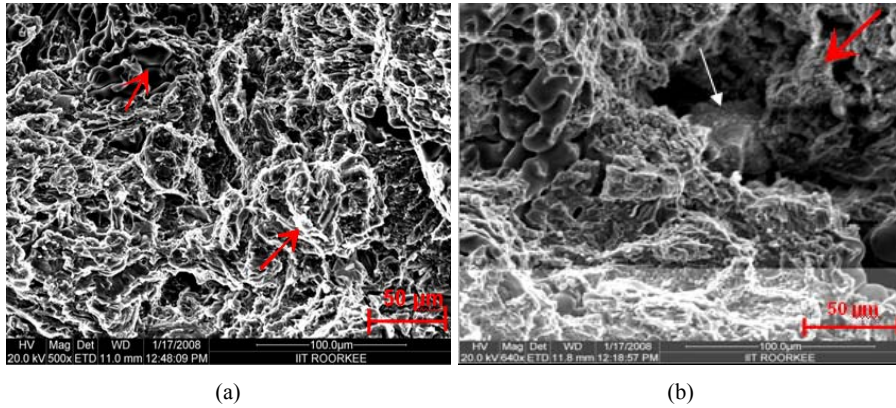
After fracture of the specimens, the fractured surfaces have been examined under SEM and characteristic features have been photographed to determine the mode of fracture and also to account for, its reasons.

Fractured surfaces of tensile specimens of AA2218-Al<sub>2</sub>O<sub>3</sub> (TiO<sub>2</sub>) composites in gravity cast and squeeze cast conditions have been studied. Typical SEM fractographs of tensile specimen of gravity cast AA2218-2 wt% Al<sub>2</sub>O<sub>3</sub> (TiO<sub>2</sub>) composite, solutionised and peak aged, is shown in Figure 4(a). One may observe dimpled ductile fracture apart from some small pores. Figure 4(b) shows typical fractograph of T61 aged gravity cast AA2218-5 wt.%Al<sub>2</sub>O<sub>3</sub> (TiO<sub>2</sub>) composite, which reveals dendrites in a shrinkage cavity, common in cast composites.

Particle-matrix de-bonding at the surface of large Al<sub>2</sub>O<sub>3</sub> particle is marked by an arrow in Figure 4(b). There are regions of dimpled ductile fracture as well. Comparative analysis of average number of dimples and average size of dimples in composites synthesised with addition of 2 and 5 wt% of blended powder is shown in Figures 5(a) and 5(b). It is observed that the average number of dimples increases and the average size of each dimple decreases with increasing addition of blended particles from 2 to 5 wt%. The fractured surface of the composites indicates that there is increase in the

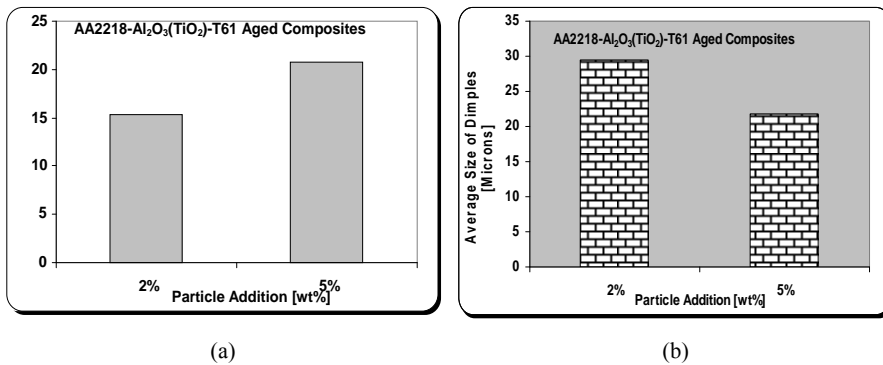
number of dimples and decrease in their size with increasing addition of particles as observed in Figure 5. Since the dimples result from the growth of voids created by de-bonding of particles from the matrix, so more particles result in more voids and at the same time, the extent of growth decreases due to reduced ductility.

**Figure 4** Shows typical SEM fractographs of tensile specimen of gravity cast AA2218- $\text{Al}_2\text{O}_3$  ( $\text{TiO}_2$ )-T61 composites tested at ambient temperature, (a) with addition of 2 wt% blended particles and (b) with addition of 5 wt% blended particles, showing partial dendrite solidification (see online version for colours)



Notes: Particle-matrix de-bonding at the surface of large  $\text{Al}_2\text{O}_3$  particle is marked by an arrow. Bright lines reflect the fracture paths.

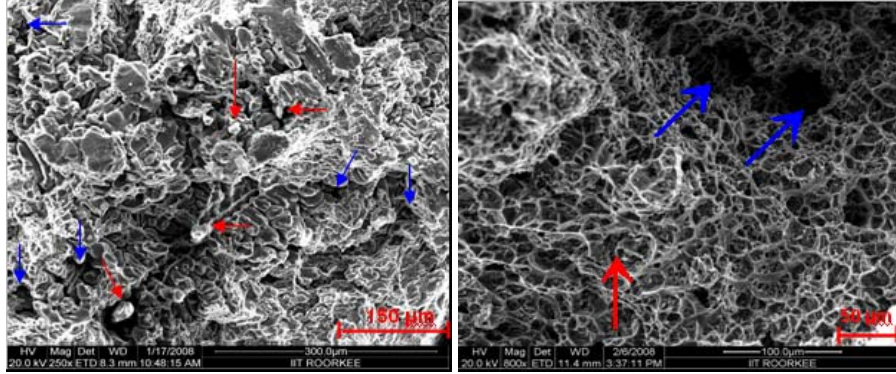
**Figure 5** (a) Shows average number of dimples in composites synthesised with addition of 2 and .5 wt% blended particles and (b) average size of dimple in composites synthesised with addition of 2 and 5 wt% blended particles



A comparison of fractographs of T61 aged AA2218-5 wt%  $\text{Al}_2\text{O}_3$  ( $\text{TiO}_2$ ) composites squeeze cast at pressures, 0, 100, 140, 180, 200 and 220 MPa, respectively, is shown in Figures 6(a) to 6(e).

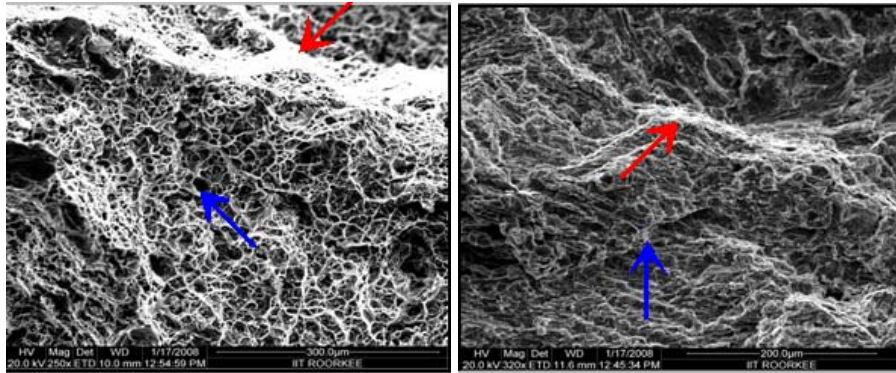


**Figure 6** Shows typical SEM pictures of fractured surfaces of tensile specimens of AA2218 5 wt%-Al<sub>2</sub>O<sub>3</sub> (TiO<sub>2</sub>)-T61 aged composite tested at ambient temperature, (a) gravity cast (b) squeeze cast at 100 MPa (c) squeeze cast at 140 MPa (d) squeeze cast at 180 MPa and (e) squeeze cast at 220 MPa (see online version for colours)



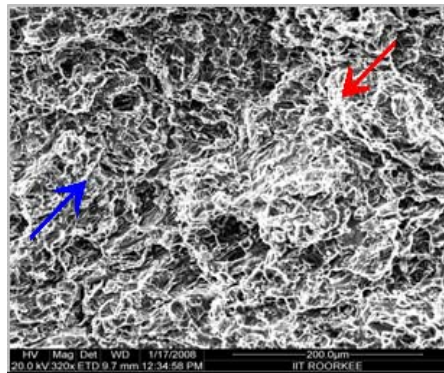
(a)

(b)



(c)

(d)



(e)

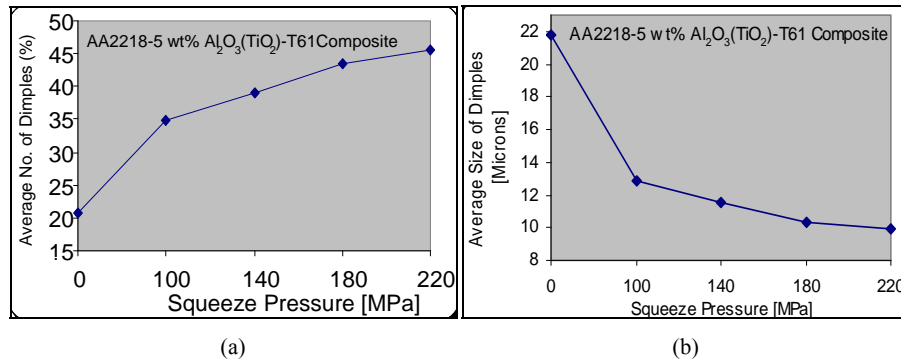


Shrinkage cavity and pores, commonly observed in gravity cast composites synthesised with higher addition of particles as in Figure 6(a), decreases considerably with application of squeeze pressure as shown in Figure 6(b). The areas under dimpled fracture are considerably more although there are two cavities possibly originating from de-bonded large alumina particles, which have come out after fracture as shown in Figure 6(b).

Some oxide particles are also observed sticking to cavities in the fractured surface shown in Figure 6(a). On comparing the fractographs, it is observed that, on increasing the squeeze pressure, the dimples in the matrix alloy are getting reduced in size and the de-bonded surface of the oxide particles, particularly from the smaller ones, are becoming increasingly prominent with increasing squeeze pressure in Figures 6(c) to 6(e).

The variation of average number of dimples and average size of dimple in AA2218-5 wt%  $\text{Al}_2\text{O}_3$  ( $\text{TiO}_2$ )-T61 aged composite, as a function of squeeze pressure is plotted in Figures 7(a) and 7(b). An increase in the number of dimples and decrease in their size is observed as the squeeze pressure is increased. There is significantly higher increase in number of dimples and also reduction in the size of dimple in between squeeze pressure of 0 and 100 MPa, as evident also from the microstructures in Figures 7(a) and 7(b).

**Figure 7** (a) Shows variation of average number of dimples and (b) shows average dimple size in microns, as a function of squeeze pressure in AA2218 5 wt%  $\text{Al}_2\text{O}_3$  ( $\text{TiO}_2$ )-T61 aged composite, tested at ambient temperature (see online version for colours)

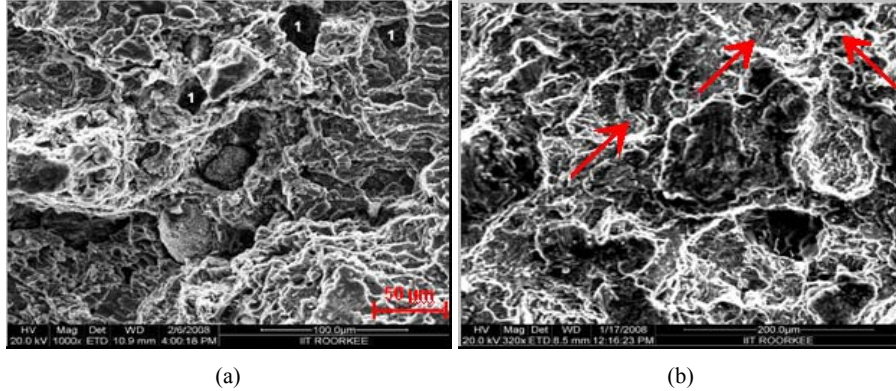


This may be attributed to more particles within the dendrite cells, which are giving rise to more voids and dimples.

But the particles in the relatively brittle interdendritic region may not originate dimples as these regions may not undergo much deformation as required for the growth of voids.

The effect of increasing test temperature on the fractured surface of AA2218-5 wt%  $\text{Al}_2\text{O}_3$  ( $\text{TiO}_2$ )-T61 aged composites squeeze cast at 100 MPa has been revealed in Figure 8. The fractured surface of the specimen tested at ambient temperature is shown in Figure 8(a) and that for the specimen tested at 400°C is shown in Figure 8(b). In Figure 8(a), dimpled region, along with voids left behind by the de-bonded large particles, marked by '1' is observed. The mode of fracture is ductile due to large number of small dimples. It is also seen that there are some dimples within a bigger dimple and particles are seen sitting at the bottom of the dimples, typical of the ductile fracture.

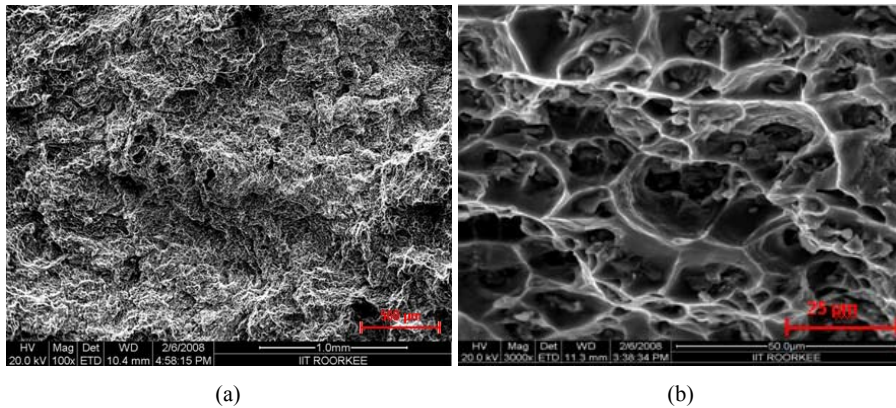
**Figure 8** Shows typical SEM pictures of fractured surface of tensile specimens of squeeze cast (100 MPa) AA2218 5wt% Al<sub>2</sub>O<sub>3</sub> (TiO<sub>2</sub>)-T61 aged composite, tested at, (a) ambient temperature, dimpled surface indicating ductile mode of fracture with signature of de-bonded particles marked by '1' and (b) at 400°C, vacant seats of de-bonded particles pulled out by other parting surface (see online version for colours)



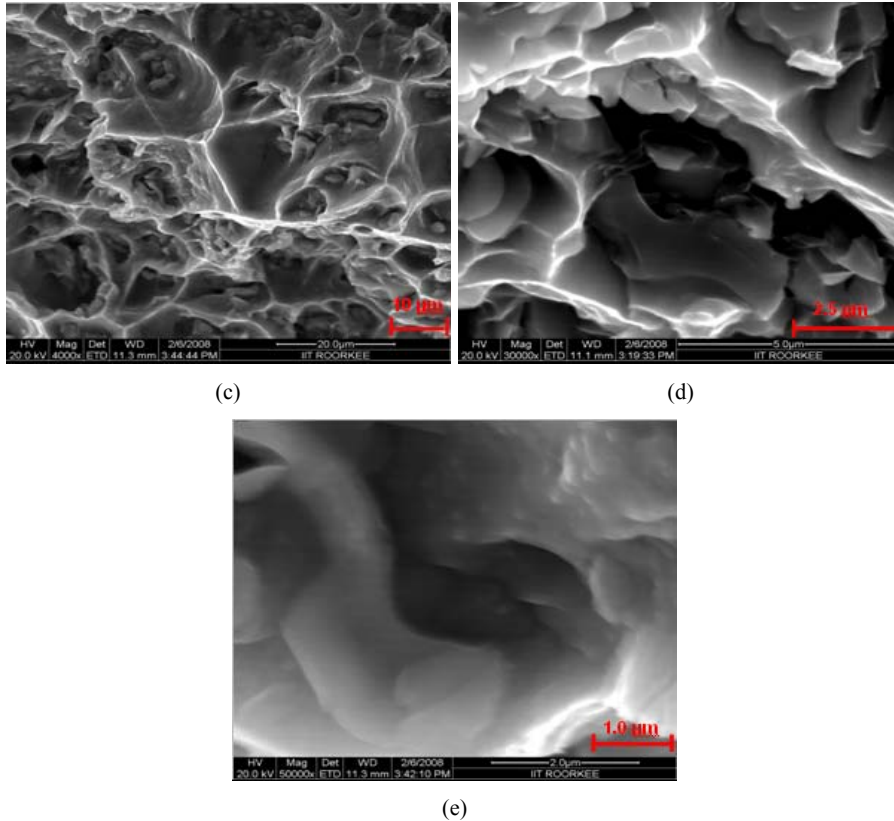
In Figure 8(b), the dimples have increased in size indicating larger ductility, leading to larger growth of voids, prior to nucleation of cracks. The average size of dimples progressively increases as the test temperature is increased. A rough estimate of the average size of dimples shows that at ambient test temperature, dimples range between 10–20 µm as observed in Figure 8(a) while the dimples obtained at 400°C test temperature range between 15–35 µm as shown in Figure 8(b).

The dimples have increased in size indicating that increased ductility at elevated temperatures help the voids to grow to a bigger size leading finally to larger dimples.

**Figure 9** Shows typical SEM pictures of fractured surfaces of tensile specimens of squeeze cast (220 MPa) AA2218 5 wt% Al<sub>2</sub>O<sub>3</sub> (TiO<sub>2</sub>)-T61 aged composite tested at 300°C, (a) a dimpled fractured surface is visible (b) dimpled surface with knife edge ridges (c) sharp ridges and typical cup and cone type of fracture (d) and (e) view of a dimple at high magnifications (see online version for colours)

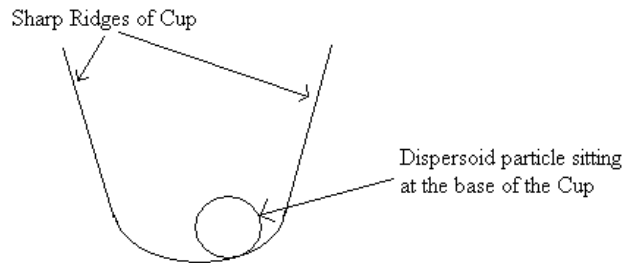


**Figure 9** Shows typical SEM pictures of fractured surfaces of tensile specimens of squeeze cast (220 MPa) AA2218 5 wt% Al<sub>2</sub>O<sub>3</sub> (TiO<sub>2</sub>)-T61 aged composite tested at 300°C, (a) a dimpled fractured surface is visible (b) dimpled surface with knife edge ridges (c) sharp ridges and typical cup and cone type of fracture (d) and (e) view of a dimple at high magnifications (continued) (see online version for colours)



Figures 9(a) to 9(e) shows typical SEM fractographs of tensile specimen of squeeze cast (220 MPa) AA2218 5 wt% Al<sub>2</sub>O<sub>3</sub> (TiO<sub>2</sub>)-T61 aged composite, tested at 300°C at different magnifications. Figure 9(a) shows dimpled fracture surface of tensile specimen at relatively lower magnification. But the dimples are clearly revealed at relatively higher magnifications in Figures 9(b) and 9(c), where one may observe small particles of oxide inclusions within the voids of the dimples. At still higher magnifications in Figures 9(d) and 9(e), one may observe clearly within the voids.

Aluminium is basically a ductile material and it has been observed that Al and its alloys exhibit ductile and semi-ductile fracture. Schematic representation of typical cup and cone fracture as observed in the fractographs, characteristic of ductile fracture, is shown in Figure 10. Particle sitting at the bottom of dimple is shown and matrix is pulled along the large distance till it is separated around the ridges. This type of fracture is commonly observed in ductile materials particularly in aluminium and its alloys.

**Figure 10** Schematic representation of cup and cone type of fracture, characteristic of ductile mode of fracture

The present investigation unravels an interesting synergy between the presence of particles and application of squeeze pressure in the context of solutionising and aging. Both the particles and the enhanced squeeze pressure contribute to refined microstructure. The particles may be contributing to refined grain size through the release of titanium by reaction of  $\text{TiO}_2$  with molten aluminium apart from the ability of reacting particles to nucleate dendrites heterogeneously, which consequently puts these particles inside dendrites and thus, there are relatively more particles inside dendrite with increasing squeeze pressure. Enhanced squeeze pressure appears to increase the ability of the particles to nucleate dendrites. The particles located in the solute rich interdendritic region acts as physical barriers to diffusion of solute, to solute deficient dendrites. Thus, there is increased dissolution of precipitates during solutionising when the particles are located inside the dendrites at higher squeeze pressure. Thus, in composites synthesised by addition of higher amount of particles, the aging response at lower squeeze pressure is less than that observed in composites synthesised with lower amounts of particles. In the context of mechanical properties, the application of squeeze pressure enhances both strength and ductility. The particles contribute to increasing strength primarily because of their role in restraining plastic flow but adversely affect ductility in spite of their contribution to grain size refinement.

#### 4 Conclusions

- 1 The microstructure of the gravity cast composites show dendrites of primary solid solution of aluminium and a number of intermetallic compounds forming in the interdendritic region due to segregation of solute and due to exceeding the solubility limit for the alloying elements in aluminium. With increasing addition of particles, there is increased tendency of particles to cluster, particularly in the interdendritic region.
- 2 Application of squeeze pressure during casting appears to make dendrite cells more round, mostly without secondary arms and the number of particles within the cells also increases with increasing squeeze pressure. Particles within the cell may be the evidence of nucleation of primary solid solution by these particles, which is also reflected in decreasing cell size.

- 3 The fractured surface of gravity cast AA2218-Al<sub>2</sub>O<sub>3</sub> (TiO<sub>2</sub>) composites indicates that there is increase in the number of dimples and decrease in their size with increasing addition of particles.
- 4 The fractured surface of squeeze cast AA2218-5 wt% Al<sub>2</sub>O<sub>3</sub> (TiO<sub>2</sub>) composites indicates that there is increase in the number of dimples and decrease in their size with increasing application of squeeze pressure.
- 5 The fracture mechanism is typically cup and cone type, characteristic of ductile fracture. But in some fractographs as the number of particles has increased, the fracture mechanism has transformed to semi-ductile from ductile, or nearly brittle in some fractographs.
- 6 By and large the fracture mechanism is ductile, in particular in specimens which are tested at higher test temperatures.

## References

- Abis, S. (1989) 'Characteristics of an aluminium alloy/alumina metal matrix composites', *Composites Science & Technology*, Vol. 35, No. 1, pp.1–11.
- Asthana, R. and Rohtagi, P.K. (1992) 'Melt infiltration of SiC compacts-I. Study of infiltration dynamics', *Zeitschrift furMetallkunde*, Vol. 83, No. 12, pp.887–892.
- Chandler, H. (1996) 'ASM heat treater's guide: practices and procedures for non-ferrous alloys', *ASM International*, Materials Park, OH.
- Curran, J.A. and Clyne, T.W. (2005) 'Thermo-physical properties of plasma electrolytic oxide coatings on aluminium', *Surface and Coatings Technology*, Vol. 199, Nos. 2–3, pp.168–176.
- Davidson, A.M. and Regener, D. (2000) 'A comparison of aluminium based metal matrix composites reinforced with coated and uncoated particulate silicon carbide', *Composites Science &Technology*, Vol. 60, No. 6, pp.865–869.
- Dunn, E.M., Wasson, R.A., Young, K.P. and Flemings, M.C. (1975) 'Growth of in-situ composites of Al-Cu-Ni alloys', *Proceeding of conference on In-Situ Composites-II*, New York.
- Hamid, A.A., Ghosh, P.K., Jain, S.C. and Ray, S. (2006) 'Processing, microstructure and mechanical properties of in-situ Al(Mg,Ti)-Al<sub>2</sub>O<sub>3</sub> (TiO<sub>2</sub>)', *Metallurgical & Material Transaction A*, Vol. 37A, No. 2, pp.469–480.
- Hanumant, G.S. and Irons, G.A. (1993) 'Particle incorporation by melt stirring for the production of metal matrix composites', *Journal of Material Science*, Vol. 28, No. 9, pp.2459–2465.
- Kang, C.G. and Yun, K.S. (1996) 'Fabrication of metal matrix composites by the die casting technique and the evaluation of their mechanical properties', *Journal of Materials Processing Technology*, Vol. 62, Nos. 1–3, pp.116–23.
- Khair, E.I. and Abou, M.T. (2005) 'Microstructure characterization and tensile properties of squeeze-cast Al-Si-Mg alloys', *Materials Letters*, Vol. 59, Nos. 8–9, pp.894–900.
- Kim, S.W., Kim, D.Y., Kim, W.G and Woo, K.D. (2001) 'The study on characteristics of heat treatment of the direct squeeze cast 7075 wrought al alloy', *Material Science and Engineering A*, Vols. 304–306, pp.721–726.
- Kumar, G., Seetharaman, S. and Gupta, M. (2014) 'Enhancing overall tensile and compressive response of pure magnesium using nano-TiB<sub>2</sub> particulates', *Material Characterization*, Vol. 94, pp.178–188.
- Lafreniene, S. and Irons, G.A. (1990) 'Sedimentation during liquid processing of metal matrix composites', *Proceeding of International Symposium on Production, Refining, Fabrication and Recycling of Light Metals*, Hamilton, Ontario, pp.177–186.



- Lampman, S.R. and Zore, T.B. (2000) 'Properties and selection of non-ferrous alloys and special purpose materials', *ASM International*, Materials Park, Ohio, pp.30, 47, 75–79(II).
- Lampman, S.R. and Zore, T.B. (2006) 'Heat treating', *ASM International*, Materials Park, Ohio, Vol. 4, pp.678, 845.
- Lawson, W.H.S. (1971) 'Mechanical behavior of rapidly solidified Al-Al<sub>2</sub>Cu and Al-Al<sub>3</sub>Ni composites', *Metallurgical Transactions.*, Vol. 2, No. 10, pp.2853–2859.
- Maity, P.C., Chakraborty, P.N. and Panigrahi, S.C. (1995) 'Processing and properties of Al-Al<sub>2</sub>O<sub>3</sub> (TiO<sub>2</sub>) in-situ particle composites', *Journal of Materials Processing Technology*, Vol. 53, Nos. 3–4, pp.857–870.
- Maity, P.C., Panigrahi, S.C. and Chakraborty, P.N. (1993) 'Preparation of aluminium-alumina in-situ particle composite', *Scripta Metallurgica et Materialia*, Vol. 28, No. 5, pp.549–552.
- Naidich, Y.V., Chubashob, Y.N., Hchunk, N.F. and Krasoskii, V.P. (1983) 'Wetting of some non-metallic materials by alumina', *Soviet Powder Metallurgy and Metal Ceramics*, Vol. 2, No. 6, pp.481–483.
- Pawlowski, L. (1995) *The Science and Engineering of Thermal Spray Coatings*, p.626, John Wiley and Sons, Inc. Oxford, UK.
- Quigley, B.F., Abbaschian, G.J., Wunderlin, R. and Mehrabian, R. (1982) 'Method for the fabrication of aluminium-alumina composites', *Metallurgical & Material Transaction A*, Vol. 13A, No. 1, pp.93–100.
- Ralph, B., Yuen, H.C. and Lee, W.B. (1997) 'The processing of metal matrix composites', *Journal of Materials Processing Technology*, Vol. 63, Nos. 1–3, pp.339–353.
- Ray, S. (1993) 'Review synthesis of cast metal matrix particulate composites', *Journal of Material Science*, Vol. 28, No. 20, pp.5397–5413.
- Sahin, Y., Kok, M. and Celik, H. (2002) 'Tool wear and surface roughness of Al<sub>2</sub>O<sub>3</sub> particle reinforced aluminium alloy composite', *Journal of Materials Processing Technology*, Vol. 128, Nos. 1–3, pp.280–291.
- Seo, Y.H. and Kang, C.G. (1995) 'The effect of applied pressure on particle dispersion characteristics and mechanical properties in melt-stirring squiz-cast SiC/AL composites', *Journal of Materials Processing Technology*, Vol. 55, Nos. 3–4, pp.370–379.
- Surappa, M.K. and Rohatgi, P.K. (1981) 'Preparation and properties of cast aluminium-ceramic particle', *Journal of Material Science*, Vol. 16, No. 4, pp.983–993.
- Tjong, S.C. and Mai, Y.W. (2008) 'Processing-structure-property aspects of particulate and whisker reinforced titanium matrix composites', *Composites Science & Technology*, Vol. 68, Nos. 3–4, pp.583–601.
- Wang, D.J. and Wu, S.T. (1994) 'The influence of oxidation on the wettability of lauminium on sapphire', *Acta Metallurgica et Materialia*, Vol. 42, No. 12, pp.4029–4034.
- Wang, X., Jha, A. and Brydson, R. (2004) 'RMD in-situ fabrication of Al<sub>3</sub>Ti particle reinforced aluminum alloy metal matrix composites', *Material Science Engineering*, Vol. A364, pp.339–345.
- Yue, T.M. (1997) 'Squeeze casting of high-strength aluminium wrought alloy AA7010', *Journal of Materials Processing Technology*, Vol. 66, Nos. 1–3, pp.179–185.
- Yue, T.M. and Chadwick, G.A. (1996) 'Squeeze casting of light alloys and their composites', *Journal of Materials Processing Technology*, Vol. 58, Nos. 2–3, pp.302–307.